Emulsion Polymerization of Isoprene. Estimation of the Branching Exponent with the Help of a Mathematical Model

Roque J. Minari,[1] Virginia I. Rodriguez,[1] Diana A. Estenoz,[1] Jorge R. Vega,[1,2] Gregorio R. Meira,[1] Luis M. Gugliotta[1]

[1]INTEC, Universidad Nacional del Litoral-CONICET, Güemes 3450, Santa Fe 3000, Argentina
[2]Facultad Regional Santa Fe, Universidad Tecnológica Nacional, Lavaisse 610, Santa Fe 3000, Argentina

ABSTRACT: This work investigates a batch and unseeded emulsion polymerization of isoprene at 10°C with *n*-dodecylmercaptan as chain transfer agent (CTA). The obtained polyisoprene (PI) was analyzed by size exclusion chromatography (SEC) with on-line viscometry. A global polymerization model was adjusted to the measurements of conversion, average particle size, and average molecular weights. The CTA concentration strongly affects the average molecular weights but has a negligible effect on conversion, average particle diameter, and average branching. Due to the combined effects of chain transfers to the polymer and to the CTA, the final molar mass distributions exhibited dispersity indexes higher than 10. The polymerization model predictions on the average degree of branching was combined with an ideal SEC model for adjusting the branching exponent of PI in tetrahydrofuran at 25°C that resulted $\varepsilon = 2.5$. A sensitivity analysis showed that +20% errors in $\overline{M}_w$ induced variations in ε lower than −10%. © 2009 Wiley Periodicals, Inc. J Appl Polym Sci 116: 590–601, 2010

Key words: polyisoprene; emulsion polymerization; GPC; molecular weight distribution; average branching

INTRODUCTION

The distributions of molecular weights (MWD) and of long chain branching (BD) of a base synthetic rubber are important characteristics that affect its processability and vulcanization. In emulsion polymerizations, such characteristics are normally controlled by addition of a chain transfer agent (CTA) and by limiting the monomer conversion to around 80%. With excessive branching, the base rubber becomes an insoluble gel.[1]

Synthetic polyisoprene (PI) is produced by anionic and Ziegler-Natta polymerizations. These rubbers are mainly 1,4-*cis* PI, which curiously is also the main microstructure of *Hevea Brasiliensis* natural rubber. Little information is available on the emulsion polymerization of isoprene (Is),[2–7] and reasons for this are the relatively large molar mass dispersities, the mixed microstructures,[2] and the higher cost of Is with respect to butadiene.[3]

Marvel and Williams[4] investigated the emulsion polymerization of Is at 50°C with $K_2S_2O_8$ as initiator and 0.3% of a mercaptan as CTA. At 75% conversion, the polymer exhibited a weight-average molecular weight ($\overline{M}_w$) of about 150,000 g/mol. Sheinker and Medvedev[5] described a similar emulsion process at 50°C but with H_2O_2 as initiator and *N*-cetyl-pyridium bromide as emulsifier. The microstructure was determined by infrared (IR) spectroscopy, resulting: 65% 1,4-*trans*; 22% 1,4-*cis*; 7% 3,4-vynil; and 6% 1,2-vynil.[6] Morton et al.[7] investigated the emulsion polymerization of Is at 5 and 15°C with a potassium fatty acid soap as emulsifier and a redox initiator (diisopropylbenzene monohydroperoxide/tetraethylenepentamine). Between 30 and 60% conversion, the kinetics followed a typical zero-one system with a constant number of particles, and the final average diameter was about 45 nm. Arrhenius expressions for the propagation rate constant were determined from the evolution of conversion at different reaction temperatures. The concentration of Is in the polymer particles at room temperature was determined under saturation conditions.[7]

Three techniques are commonly used for determining the degree of long chain branching: ^{13}C-nuclear magnetic resonance (NMR) spectroscopy, multi-detection size exclusion chromatography (SEC), and IR spectroscopy. For an emulsion poly(*n*-butyl

acrylate), solid-state ^{13}C-NMR[8–11] enabled the determination of branching in a few percents of the repeating units. Solid-state ^{13}C-NMR is less sensitive than solution NMR, but this last technique requires full solubility without the presence of gel. For a branched polyolefin, high-resolution melt-state NMR with magic-angle spinning (MAS) enabled to quantify branching as low as 0.001% of the repeating units.[12–14] More recently, melt-state MAS NMR was adapted for characterizing randomly-branched polyacrylates with degrees of branching of around 2% of the repeating units.[15] Even though ^{13}C-NMR cannot normally discriminate between long and short branches, with some polyolefins it has been possible to distinguish short branches with up to 6 carbons.[12,13]

For long chain-branched homopolymers, SEC fitted with a differential refractometer (DR) and a specific viscometer (SV) enables to simultaneously determine the MWD and branching distribution.[16] For these systems, Guaita and Chiantore[17] concluded that errors in the sample concentrations induce proportional errors in the average molecular weights and in the Mark-Houwink-Sakurada (MHS) constant K, but do not affect the MWD shape or the slope α of the MHS plot. A branched homopolymer is more compact than a linear homologue of the same molar mass. The branching parameter g (≤ 1) is defined by $(S^2)_b/(S^2)_l$ with $M_b = M_l$, where (S^2) is the squared average radius of gyration, M is the molar mass, and the subscripts "b" and "l" indicate branched and linear polymer, respectively.[18,19] Assuming ideal fractionation according to molar mass, the Zimm-Stockmayer eq. (1)[18] is applied to the instantaneous SEC fractions of homopolymers containing long trifunctional branches. Calling V the elution volume, $g(V)$ is related to the instantaneous number-average number of branches per molecule $B_{n3}(V)$ through:

$$g(V) = \left[\left(1 + \frac{B_{n3}(V)}{7} \right)^{1/2} + \frac{4B_{n3}(V)}{9\pi} \right]^{-1/2} \leq 1 \quad (1)$$

As $g(V)$ is difficult to evaluate, then the following alternative g' branching parameter was introduced:

$$g'(M) = \frac{[\eta]_b(M)}{[\eta]_l(M)} = \frac{[\eta]_b(M)}{K M^\alpha} \leq 1 \qquad (M_b = M_l = M)$$

$$(2)$$

where $[\eta]_b$ and $[\eta]_l = K M^\alpha$ are the intrinsic viscosities of the branched and linear homologue, respectively.[20] The two branching parameters are interrelated through the empirical expression:

$$g' = g^\varepsilon \qquad (3)$$

where the ε exponent is only known for a few polymer–solvent systems,[21] and it was seen to depend

on the molar mass.[22,23] Replacing eq. (2) into eq. (3), one obtains:

$$g(M) = \left[\frac{[\eta]_b(M)}{K M^\alpha} \right]^{\frac{1}{\varepsilon}} \qquad (4)$$

Even though according to theory $0.5 < \varepsilon < 1.5$, values of ε larger than 1.5 have also been reported.[22–24] Thus, $\varepsilon = 2$ was indirectly estimated for a styrene-butadiene graft copolymer in tetrahydrofuran (THF) at ambient temperature, and to this effect, SEC measurements with on-line viscometry were combined with estimates from a polymerization/ideal SEC model.[22] Even though such estimates of ε are not necessarily accurate from the physicochemical point of view, they are useful for adjusting model predictions to SEC measurements. Tackx and Tacx[23] used SEC with on-line multi-angle laser light-scattering for estimating the ε values of low-density polyethylenes (LDPEs). They determined that ε ranged from 1.2 to 1.8 for autoclave products and from 1.0 to 1.5 for tubular products.[23] Kühn et al.[24] determined $\varepsilon = 1.2$ for an autoclave LDPE in 1,2,4-trichlorobenzene at 135°C and $\varepsilon = 2.0$ for the equivalent tubular material. As far as the authors are aware, there are so far no published values of ε for THF solutions of emulsion PI.

Unfortunately, SEC/viscometry only provides semiquantitative estimates of the distributions of chain branching. This is because: (a) although the Zimm-Stockmayer eq. (1) was developed for molecules of equal M, it is applied to molecules eluting at equal V's; (b) intrinsic viscosities measurements are poor at the chromatogram tails and at low molar masses; (c) errors in the intervening parameters such as ε, α, and K are transferred into the results; and (d) a final data processing is required to transform the continuous BD derived from the SEC measurements into the true discrete BD $W(B_{n3})$, where W indicates mass fraction and B_{n3} are integer values. A global average number of branches per molecule $(\overline{B}_{n3})$ can be determined from the mass chromatogram $w(V)$ and the $B_{n3}(V)$ function given by eq. (1), through:

$$\overline{B}_{n3} = \frac{\sum B_{n3}(V) \, w(V) \, M(V)^{-1}}{\sum w(V) \, M(V)^{-1}} \qquad (5)$$

where $M(V)$ is the molecular weight calibration of the analyzed polymer.

In this work, three batch emulsion polymerizations of Is at 10°C were carried out, and a global polymerization model was adjusted to measurements of monomer conversion, particle diameter, and average molecular weights. Then, SEC/viscometry measurements were combined with predictions from the polymerization model to estimate a global ε exponent for PI in THF at ambient temperature.
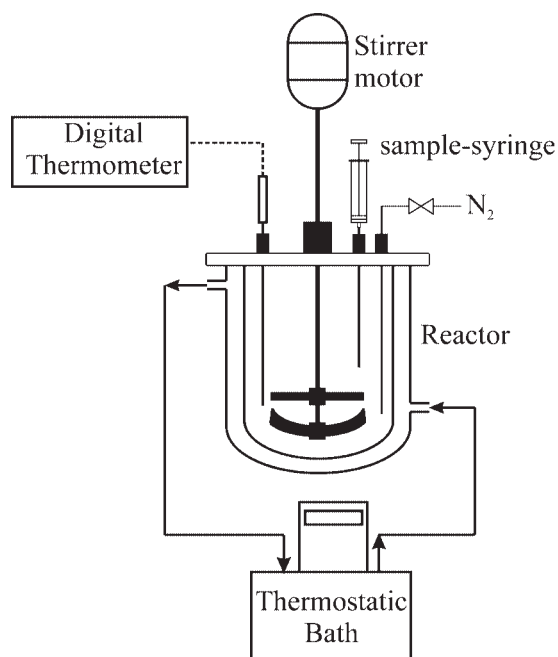
Figure 1 The reaction system (schematic).

EXPERIMENTAL WORK

Materials

The following reagents were used as received: (a) sodium lauryl sulfate (SLS) emulsifier (Mallinckrodt, purity 95%); (b) *n*-dodecyl mercaptan (*n*DM) CTA (Fluka AG); (c) *p*-menthane hydroperoxide (PMHP) initiator (purity 54%); (d) $FeSO_4.7H_2O$ oxidating agent (purity 20%); (e) sodium formaldehyde sulfox-ilate (SFS) reducing agent (purity 98%); and (f) ethylenediaminetetraacetic acid (EDTA) buffer (purity 40%). The Is (Aldrich, gold level) was washed several times with a 15% KOH solution to eliminate the inhibitor, washed with water until neutral pH, and dried with $CaCl_2$.

Distilled and deionized water was used throughout the work.

Polymerizations and characterization

Three batch polymerizations of Is were carried out using the reaction system that is schematized in Figure 1. It included a 1 L-glass reactor equipped with a modified anchor stirrer at 250 rpm, a sampling system, a digital thermometer, and a N_2 inlet. The temperature was controlled with a thermostatic bath. Polymerizations were carried out at 10°C, with a PMHP/$FeSO_4$/SFS redox initiation system, and *n*DM as CTA. The three reactions mainly differed in the initial concentration of CTA (see recipes in the upper half of Table I).

The reactions were as follows. First, the emulsifier and 390 g of water were loaded into the reactor. Then, the temperature was stabilized at 10°C; the monomer, CTA, and initiator were loaded; and the mixture was stirred for 30 min under continuous N_2 bubbling. The polymerization was started when loading a water solution of $FeSO_4.7H_2O$, SFS, and EDTA. Along the reactions, N_2 bubbling was maintained and samples were withdrawn. The following measurements were carried out in our laboratories onto the withdrawn samples: (i) the total monomer

TABLE I
Batch Experiments 1–3. Recipes and Characteristics of the Final Latex Samples. In all Cases, the Reaction Temperature was 10°C, and the Stirring Rate was 250 rpm

(a) Recipe (in pphm[a])	Exp. 1	Exp. 2	Exp. 3
Monomer (Is)	100	100	100
CTA (*n*DM)	1.55	0.83	0.49
Initiator (PMHP)	0.073	0.070	0.069
Oxidant ($FeSO_4.7H_2O$)	0.034	0.034	0.034
Reducing agent (SFS)	0.10	0.10	0.10
Buffer (EDTA)	0.09	0.09	0.09
Emulsifier (SLS)	11.76	11.77	11.67
Water	399.9	398.6	395.2

		Exp. 1		Exp. 2		Exp. 3	
(b) Final sample characteristics		Meas.	Sim.	Meas.	Sim.	Meas.	Sim.
x	[%]	84.6	82.6	86.5	83.2	87.2	83.5
$\overline{d}_p$	[nm]	27.4	26.9	30.2	27.5	29.2	27.8
$\overline{M}_n$	[g/mol]	25400	37700	71700	65200	71200	103000
$\overline{M}_w$	[g/mol]	262000	298000	742000	562000	891000	852000
$\overline{M}_w/\overline{M}_n$	[–]	10.3	7.9	10.3	8.6	12.5	8.3
$\overline{B}_{n3}$	[molec^{-1}]	0.32	0.37	0.32	0.42	0.35	0.44
$\overline{B}_{n4}$	[molec^{-1}]	–	6.7×10^{-7}	–	1.3×10^{-6}	–	2.6×10^{-6}

[a] Parts per hundred monomer.

conversion x was determined by gravimetry; (ii) the unswollen average particle diameter $\bar{d}_p$ was determined with a Brookhaven BI-9000 AT dynamic light scattering (DLS) photometer; and (iii) the MWD was determined with a Waters 1515 chromatograph fitted with 6 μ-Styragel columns and a Viscotek 200 detector (i.e.: containing a SV in parallel with a DR). Each latex sample was subdivided into three fractions. The first fraction was dried at 80°C until constant weight for measuring conversion. The second fraction was diluted with water before measuring particle size. The third fraction was treated as follows for the SEC characterization: (a) a commercial antioxidant [4,6-bis (octylthiomethyl)-o-cresol] was added into the latex to avoid degradation; (b) the latex was precipitated in isopropanol; and (c) the precipitate was filtered, dried under vacuum, and stored in the dark at −15°C until analysis. None of the samples showed evidence of gel.

SEC analysis

Figure 2 presents the baseline-corrected DR and SV chromatograms at three different conversions for Exp. 1(a,d), Exp. 2(b,e) and Exp. 3(c,f). A linear concentration calibration was obtained from DR measurements by correlating accurately known masses of injected PI standards with their corresponding chromatogram areas. Also, a "universal" molecular weight calibration ($\log([\eta]M) = 18.828 - 0.335\ V$),

was obtained from a set of nine narrow PS standards in the range 50,000–3,000,000 g/mol. The data analysis involved first calculating the intrinsic viscosity measurements $[\eta]_b(V)$ from the ratio between the SV measurements and the mass concentration. Then, the instantaneous molecular weights $M(V)$ were estimated from the universal calibration and $[\eta]_b(V)$. Finally, the MWDs were determined from $M(V)$ and the concentration chromatogram.

For calculating $B_{n3}(V)$, the following information is required [eqs. (1,4)]: $[\eta]_b(V)$, $M(V)$, and the parameters K, α, and ε for PI in THF at ambient temperature. Unfortunately, the value of ε was unknown. To a first approximation, the MHS parameters were estimated from 3 narrow anionic PI standards (Polysciences, in the range 30,000–300,000 g/mol); yielding: $K = 1.96 \times 10^{-4}$ dL/g, and $\alpha = 0.734$. These values almost coincide with previous estimates by Jackson et al.[25] ($K = 1.95 \times 10^{-4}$ dL/g, and $\alpha = 0.73$); but somewhat differ from older determinations by Tung[26] ($K = 1.49 \times 10^{-4}$ dL/g, and $\alpha = 0.745$).

Experimental results

The measurements are presented in the lower half of Table I and in Figures 3 and 4. Figure 3 shows the time evolution of monomer conversion, average particle diameter ($\bar{d}_p$), and average molecular weights ($\overline{M}_n$ and $\overline{M}_w$) (in symbols). Figure 4 presents the MWDs at three different reaction times. In such Figures, "accumulation" peaks or elbows are observed at M's $> 10^6$ g/mol; possibly caused by a low column resolution at the high molar mass end. Table I presents the final latex characteristics. The following is observed in all three experiments: (a) the final conversions are close to 85%; (b) the initial CTA concentration strongly affects the average molecular weights but exhibits only a minor effect on x and $\bar{d}_p$; (c) the average molecular weights fall along the reactions; and (d) the MWDs become broader with conversion (Fig. 4), reaching final dispersities above 10 (Table I).

MATHEMATICAL MODEL AND SIMULATION RESULTS

The mathematical model is presented in the Appendix. Even though it has not been previously reported, it was obtained by simplifying a more detailed model by Gugliotta et al.[27] for the emulsion copolymerization of styrene and butadiene. The kinetic mechanism is given in Table II. It considers initiation and propagation in the aqueous phase; and the following reactions in polymer phase: propagation, termination, chain transfers (to the CTA, monomer, and polymer), and reactions with internal double bonds (propagation to the polymer). To calculate
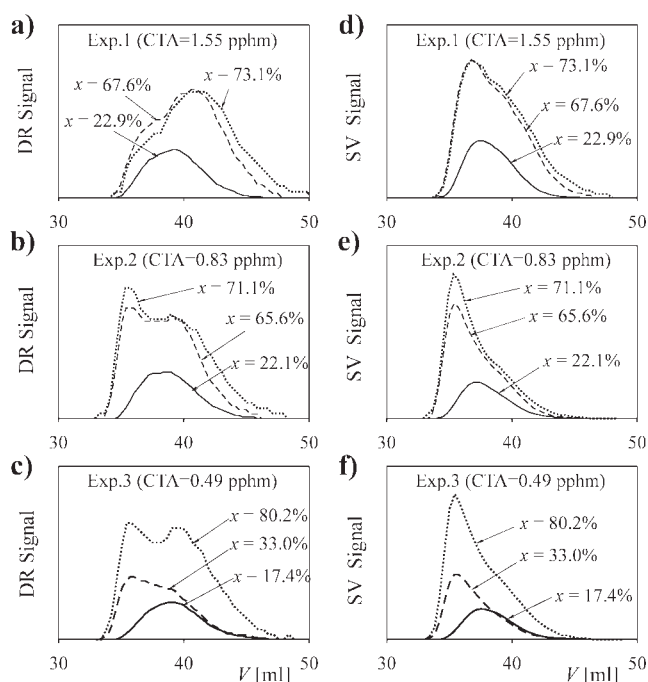

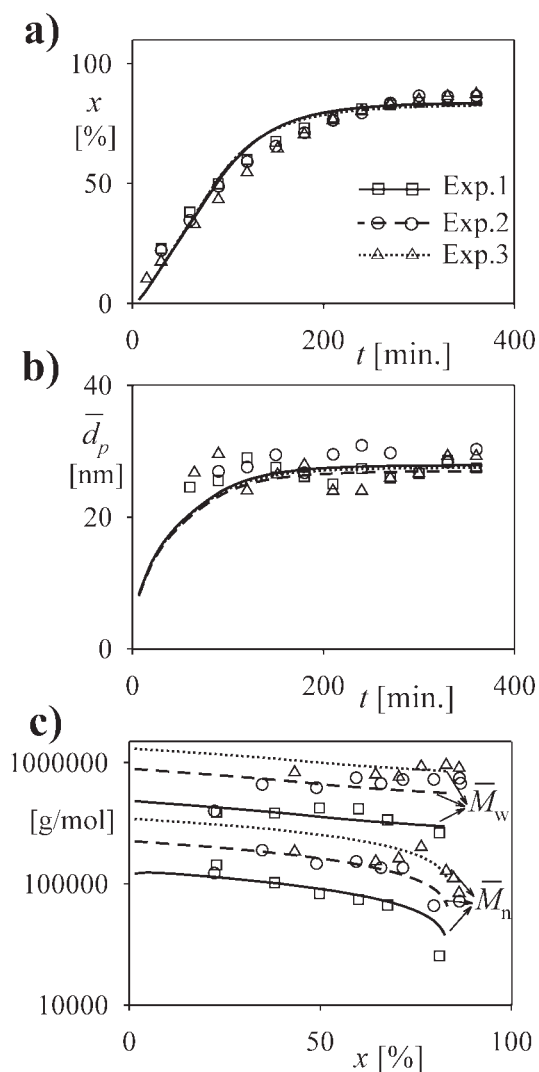**Figure 2** Experiments 1–3. Baseline-corrected (DR and SV) chromatograms.

Figure 3 Experiments 1–3. Measurements (in symbols) and model predictions (in trace) of the monomer conversion (a); the average particle diameter (b); and the average molecular weights (c).

the MWD, a pseudobulk model was adopted in the polymer phase. The main model hypotheses are: (a) polymer particles are only generated by micellar nucleation; (b) free-radicals reach pseudosteady states in both the aqueous and polymer phases; (c) termination is negligible in the aqueous phase; (d) the monomer is only consumed by propagation in the polymer phase; (e) the particle size distribution is uniform; (f) the monomer and the CTA are distributed among the phases according to equilibrium with constant partition coefficients; (g) the desorption coefficient of primary CTA radicals from the polymer particles into the aqueous phase is estimated following Nomura et al.[28]; (h) in the polymer phase, all the propagating radicals exhibit a common reactivity; (i) long trifunctional branches are generated by chain transfer to the polymer; (j) long tetrafunctional branches are generated by reaction with

Journal of Applied Polymer Science DOI 10.1002/app

internal double bonds; and (k) short branches generated by backbiting reactions are neglected.

Parameter adjustment

The model parameters are presented in Table III. Most of the parameters were directly taken from the literature. The monomer partition coefficients between the monomer droplets phase (d) and the water phase (w) (K_{Isdw}) and between the water phase and the polymer phase (p) (K_{Iswp}) were estimated from the following expressions, assuming saturation conditions:

$$K_{Isdw} = \frac{\rho_{Is}/M_{Is}}{[Is]_w^{sat}} \tag{6}$$

$$K_{Iswp} = \frac{[Is]_w^{sat}}{[Is]_p^{sat}} \tag{7}$$

where ρ_{Is} is the monomer density, M_{Is} is the monomer molar mass, $[Is]_p^{sat} = 5.3$ mol/L is the monomer
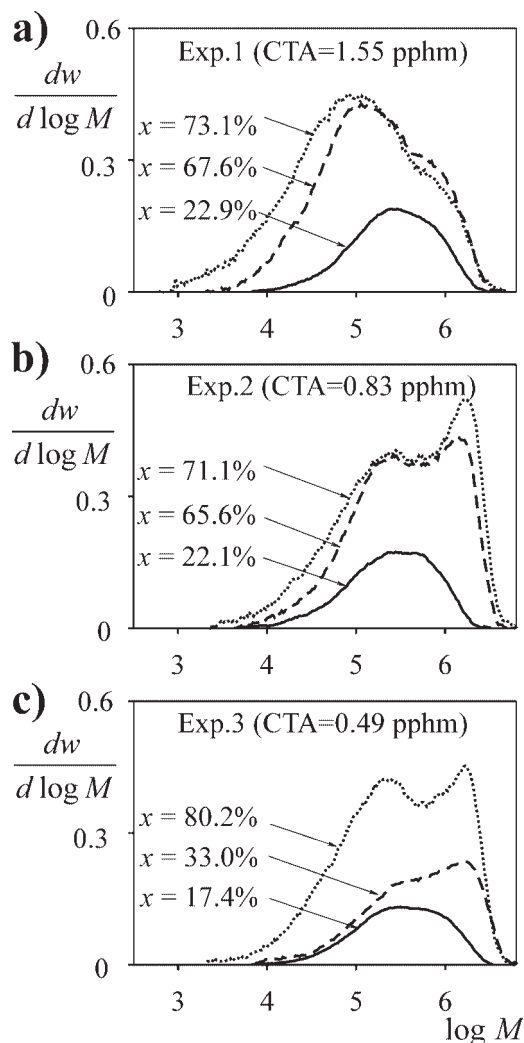

Figure 4 Experiments 1–3. MWDs obtained by SEC at three different conversions.

TABLE II
Global Kinetics

	Polymer Phase (n, m = 1, 2,...)	Aqueous Phase (n = 1, 2,...)
Initiation	–	$I + Fe^{2+} \xrightarrow{k_1} R_c^\bullet + Fe^{3+} + OH^-$
		$Fe^{3+} + Ra \xrightarrow{k_2} Fe^{2+} + Ra^+$
		$R_c^\bullet + Is \xrightarrow{k_{pc}} R_{(1)_w}^\bullet$
Propagation	$R_{(n)}^\bullet + Is \xrightarrow{k_p} R_{(n+1)}^\bullet$	$R_{(n)_w}^\bullet + Is \xrightarrow{k_{pw}} R_{(n+1)_w}^\bullet$
Termination Reactions	$R_{(n)}^\bullet + R_{(m)}^\bullet \xrightarrow{k_{tp}} P_{(n+m)}$	–
	$R_{(n)}^\bullet + R_{(m)}^\bullet \xrightarrow{k_{tp}} P_{(n)} + P_{(m)}$	
Chain Transfer to the Monomer	$R_{(n)}^\bullet + Is \xrightarrow{k_{fM}} P_{(n)} + R_{(1)}^\bullet$	–
Chain Transfer to the CTA	$R_{(n)}^\bullet + X \xrightarrow{k_{fX}} P_{(n)} + X^\bullet$	–
Chain Transfer to the Polymer	$R_{(n)}^\bullet + P_{(m)} \xrightarrow{k_{fP}} P_{(n)} + R_{(m)}^\bullet$	–
Propagation to the Polymer	$R_{(n)}^\bullet + P_{(m)} \xrightarrow{k_p^*} R_{(n+m)}^\bullet$	–

concentration in the polymer particles under saturation conditions[7]; and $[Is]_{tw}^{sat} = 4.3 \times 10^{-3}$ mol/L is the water solubility of Is.[32] The CTA partition coefficient (K_{Xdw}) was estimated from the water solubility of nDM at 60°C as reported by Song and Poehlein[33] ($[X]_w^{sat} = 3 \times 10^{-5}$ mol/L) and:

$$K_{Xdw} = \frac{\rho_X / M_X}{[X]_w^{sat}} \quad (8)$$

where ρ_X and M_X are, respectively, the CTA density and molar mass. For the emulsion polymerization of styrene, Nomura et al.[34] found that linear mercaptans with between 7 and 12 C atoms distribute them-

selves between the polymer particles and the monomer droplets similarly to the monomer. For our Is-X system, we assumed a similar behavior, i.e.:

$$K_{Xwp} = \frac{K_{Isdw} K_{Iswp}}{K_{Xdw}} \quad (9)$$

The model parameter adjustment involved the sequential minimization of three average errors. In a first stage, the following three parameters were adjusted: (i) the ratio between the mass transfer resistance of CTA radicals on the water side and the overall mass transfer resistance (δ); (ii) the area covered by a mol of emulsifier (A_S); and (iii) the rate constant for generation of primary free

TABLE III
Model Parameters of an Emulsion Polymerization of Is at 10°C with nDM as CTA

Model parameter	Value	Ref.
D_{Xw}	2.29×10^{-6} dm^2 min^{-1}	Wilke and Chang[29]
$[E]_{CMC}$	9.00×10^{-3} mol dm^{-3}	Harelle et al.[30]
K_{Isdw}	2.27×10^3	eq. (6)
K_{Iswp}	8.31×10^{-4}	eq. (7)
K_{Xdw}	1.41×10^5	eq. (8)
K_{Xwp}	1.33×10^{-5}	eq. (9)
K_{Idw}	1.38×10^3	Gugliotta et al.[27]
K_{Iwp}	7.25×10^{-4}	Gugliotta et al.[27]
ρ_p	9.13×10^2 g dm^{-3}	Brandrup and Immergut[31]
δ	1.58×10^{-2}	Adjusted in this work
A_S	3.69×10^7 dm^2 mol^{-1}	Adjusted in this work
k_1	1.09×10^3 dm^3 mol^{-1} min^{-1}	Adjusted in this work
k_2	2.50×10^1 dm^3 mol^{-1} min^{-1}	Gugliotta et al.[22]
k_{fM}	3.47×10^{-2} dm^3 mol^{-1} min^{-1}	Adjusted in this work
k_{fX}	1.032×10^1 dm^3 mol^{-1} min^{-1}	Adjusted in this work
k_{fP}	$[6.66 \times 10^{-2} - 4.99 \times 10^{-8} \overline{M}_w^a]$ dm^3 mol^{-1} min^{-1}	Adjusted in this work
k_p^*	6.93×10^{-10} dm^3 mol^{-1} min^{-1}	Adjusted in this work
k_p	1.94×10^2 dm^3 mol^{-1} min^{-1}	Morton et al.[7]
k_{tp}	2.55×10^6 dm^3 mol^{-1} min^{-1}	Gugliotta et al.[22]

^{a} value at final conversion.

radicals (k_1). To this effect, the following expression was applied:

$$\min_{\delta, A_S, k_1} E_1 = \frac{1}{S} \sum_s$$

$$\times \left[\frac{(x_{\text{exp.}}(s) - x_{\text{theor.}}(s))^2}{x_{\text{exp.}}^2(s)} + \frac{(\overline{d}_{p,\text{exp.}}(s) - \overline{d}_{p,\text{theor.}}(s))^2}{\overline{d}_{p,\text{exp.}}^2(s)} \right] \quad (10)$$

where the subscripts "exp." and "theor." indicate measured and simulated values, respectively; s indicates sample number; and S is the total number of samples.

In a second stage, the rate constants of chain transfer to the CTA (k_{fX}), of chain transfer to monomer (k_{fM}), and of propagation to the polymer (k_p^*) were simultaneously adjusted to fit the measurements of $\overline{M}_n$ through:

$$\min_{k_{fX}, k_{fM}, k_p^*} E_2 = \frac{1}{S} \sum_s \left[\frac{(\overline{M}_{n,\text{exp.}}(s) - \overline{M}_{n,\text{theor.}}(s))^2}{\overline{M}_{n,\text{exp.}}^2(s)} \right] \quad (11)$$

In a third stage, the chain transfer constant to the polymer (k_{fP}) was adjusted to fit the measurements of $\overline{M}_w$. In this case, constant but different values of k_{fP} were adjusted onto each reaction, according to their final $\overline{M}_w$. More specifically, a linear relationship between k_{fP} and $\overline{M}_w$ was imposed, to consider the effect of the molar mass on the "diffusion-controlled" transfer reactions involving a macroradical and an accumulated polymer molecule. The following functional was used:

$$\min_{k_{fP}} E_3 = \frac{1}{S} \sum_s \left[\frac{(\overline{M}_{w,\text{exp.}}(s) - \overline{M}_{w,\text{theor.}}(s))^2}{\overline{M}_{w,\text{exp.}}^2(s)} \right] \quad (12)$$

Model results

The final model predictions are in Figures 3 and 5. The predicted evolutions of x and $\overline{d}_p$ adequately adjust the experimental data [Fig. 3(a,b); and Table I]. The small particle diameters of Figure 3(b) ($\overline{d}_p \sim$ 30 nm) and the low water solubilities of the monomer and CTA suggest a Case 2 Smith-Ewart's kinetics, with an average number of radicals per particle $\overline{n} = 0.5$. Figure 3(c) shows that the molecular weights decrease for increasing CTA concentrations. Notice that since the model parameters were adjusted by minimizing a global difference between measurements and predicted average molecular weights, this may produce both over- and underestimations of the measured values, which is observed in Figure 3(c) and Table I. The decrease in $\overline{M}_n(t)$ is
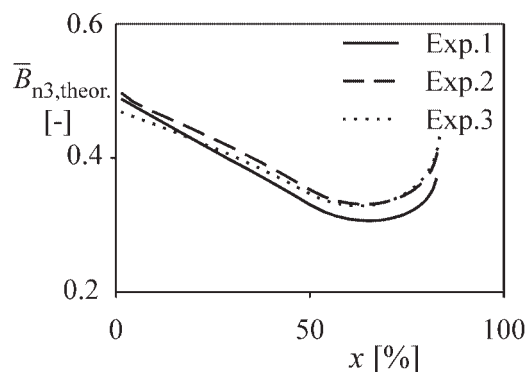
Figure 5 Model predictions for the global number-average number of trifunctional branches per molecule ($\overline{B}_{n3,\text{theor.}}$).

indicative that $C_X = k_{fX}/k_p < 1$. Thus, the ratio between the CTA and the monomer in the polymer particles, $[X]_p(t)/[Is]_p(t)$, increases along the reaction. The MWDs broaden with conversion due to the combination of two effects: $\overline{M}_w$ increases with chain branching, and $\overline{M}_n$ decreases for increasing CTA:monomer ratio.

According to the model, the final average number of trifunctional branches $\overline{B}_{n3}$ is around 5 orders of magnitude higher than the average number of tetrafunctional branches per molecule ($\overline{B}_{n4}$) (Table I). Thus, only trifunctional branches were assumed in the SEC data treatment. Notice that at the final conversions, the model predicts average branches per molecule lower than 1. Thus, highly branched PI (HBPI) is not generated under the applied operation conditions.

Also according to the model, $\overline{B}_{n3}$ reaches a minimum at around 70% conversion (Fig. 5). This minimum is explained as follows. Although monomer droplets are still present (up to about 50% conversion), the weight fraction of polymer in the polymer particles remains essentially constant, and this results in a constant generation of long chain branches. In addition, the reduction in $\overline{M}_n$ increases the molar concentration of polymer in the polymer particles, thus reducing $\overline{B}_{n3}$. After disappearance of the monomer droplets, the weight fraction of polymer in the polymer particles monotonically increases, and the rate of generation of branches increases. As this last rate increases more rapidly than [CTA]/[Is], this generates a minimum in $\overline{B}_{n3}$.

ε EXPONENT FOR PI IN THF AT ROOM TEMPERATURE

Unfortunately, standard ^{13}C-NMR could not applied[15] for quantifying the (rather low) average degrees of branching involved (<0.1% of branches per monomer unit). Instead, an optimal value of

TABLE IV
Comparison between Simulated and Experimental Average Branching (with ε = 2.5)
for the Samples Considered in the Proposed Procedure

Sample $N°$/ Exp. $N°$	Measurements				Simulations
	x [%]	$\overline{M}_n$ [g/mol]	$\overline{M}_w$ [g/mol]	$\overline{B}_{n3,\text{exp.}}$ [molec^{-1}]	$\overline{B}_{n3,\text{theor.}}$ [molec^{-1}]
1/1	22.8	143,000	391,000	0.64	0.42
2/1	73.1	66,700	337,000	0.32	0.31
3/2	34.6	189,000	658,000	0.41	0.40
4/2	71.1	135,000	670,000	0.32	0.34
5/2	86.5	71,700	742,000	0.32	0.42
6/3	17.4	109,000	370,000	0.43	0.43
7/3	80.2	90,700	654,000	0.35	0.38

ε for PI in THF at ambient temperature was estimated by comparing the "theoretical" model predictions for $\overline{B}_{n3}(x)$ presented in Figure 5 with the corresponding SEC estimates. The procedure was applied onto the seven samples listed in Table IV.

Consider first data treatment that was applied onto the SEC/viscometry measurements for estimating the "experimental" global averages of the number of branches per molecule $\overline{B}_{n3,\text{exp.}}$ on the basis of many possible values of ε in the range (0.5–3.0). Figure 6(a) presents the measurements of $\log[\eta]_b$ versus $\log M$ together with the MHS plot of the linear anionic PI standards for 3 (out of the 7) samples listed in Table IV. For evaluating the denominator of eq. (4), the MHS exponent was adopted equal to that of the PI standards (i.e., $\alpha = 0.734$). In contrast, the K constant was readjusted by vertically shifting the $\log[\eta]_b$ versus $\log M$ plots until obtaining a common average intercept [see Fig. 6(b)], yielding $K = 2.54 \times 10^{-4}$ dL/g. Possibly, the difference in the intercepts of Figure 6(a) are caused by errors in the injected sample concentrations.[9] Then, the $\overline{B}_{n3,\text{exp.}}$ values were obtained in three steps. In step 1, the $g'(\log M)$ functions were calculated through eq. (2) [Fig. 6(c)]. For these functions, an upper limit of 1 was imposed, as values higher than unity are indicative of measurement errors. In step 2, 51 possible values of ε in the range (0.5–3.0) were selected, their corresponding $g(\log M)$ functions were estimated from the $g'(\log M)$ functions of Figure 6(c); and the functions $B_{n3,\text{exp.}}(\log M)$ were obtained from $M(V)$ and the following inverted version of eq. (1):

$$B_{n3,\text{exp.}}(\log M) = 7.068\,g^{-2}(\log M) + 3.568$$
$$- \sqrt{62.7 + 50.454\,g^{-2}(\log M)} \quad (13)$$

Figures 7(a–c) present the resulting $\overline{B}_{n3,\text{exp.}}(\log M, \varepsilon)$ functions for three illustrated samples and for only three possible values of ε. In step 3, eq. (5) was applied, and for each of the seven analyzed samples,

51 possible global "experimental" averages $\overline{B}_{n3,\text{exp.}}$ were obtained.

Finally, consider the estimation of the best global value of ε. To this effect, an (averaged and
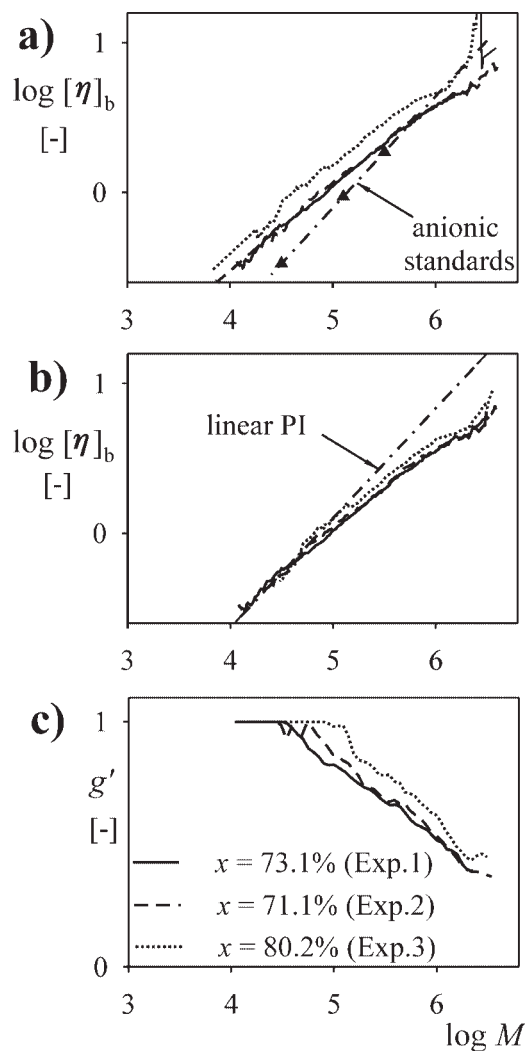

Figure 6 (a) Raw measurements of $\log[\eta]_b$ versus $\log M$ for three of the samples considered in the proposed procedure, and for three linear anionic PI standards. (b) Vertically-readjusted plots of (a); and (c) Experimental determinations of $g'(\log M)$.
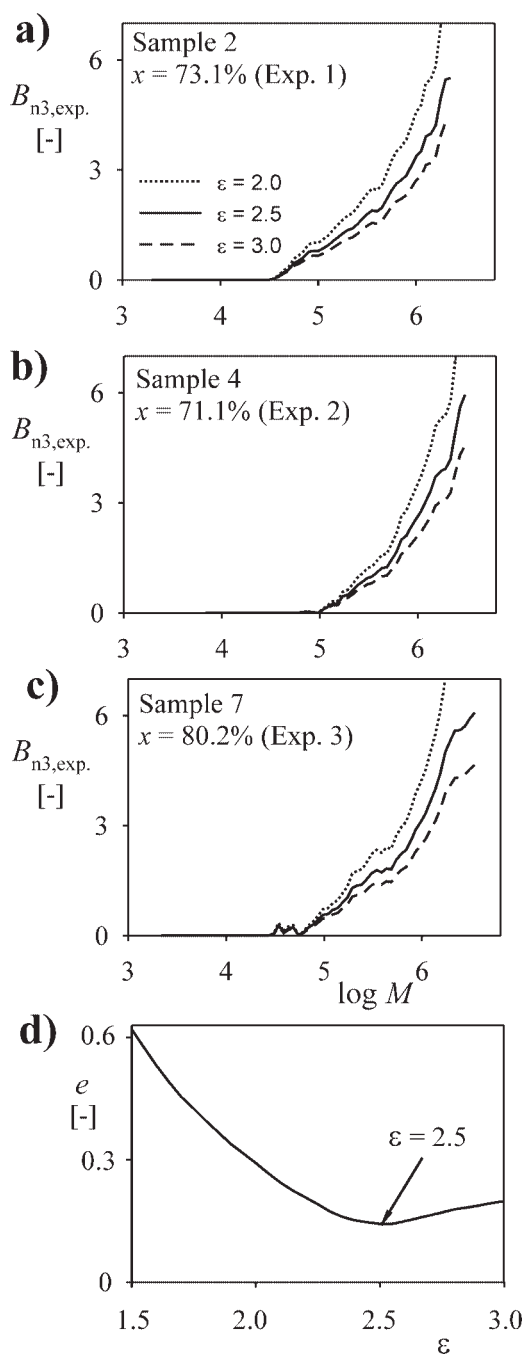
a)

b)

c)

d)

Figure 7 (a–c) Evolutions of $B_{n3,exp.}(\log M)$ for three tested values of ε; and (d) Evolution of the global error as a function of ε, also showing the finally-sought value ($\varepsilon = 2.5$).

normalized) scalar error (e) of the differences between $\overline{B}_{n3,theor.}$ as obtained from the polymerization model and its corresponding $\overline{B}_{n3,exp.}(\varepsilon)$ were minimized through:

$$\min_{\varepsilon} e = \frac{1}{7} \sum_{s} \left[\frac{\left(\overline{B}_{n3,exp.}(\varepsilon,s) - \overline{B}_{n3,theor.}(s) \right)^2}{\overline{B}_{n3,theor.}^2(s)} \right] \quad (14)$$

The procedure yielded $\varepsilon = 2.5$ [Fig. 7(d)]. For this last value, Table IV presents the final experimental estimates of $\overline{B}_{n3}$.

SENSITIVITY ANALYSIS

The polymerization model required the adjustment of seven parameters. However, the theoretical estimates of $\overline{B}_{n3}$ (and therefore the final estimate of ε) mainly depend on the values of the chain transfer to the polymer k_{fp}, that was adjusted on the basis of the measurements of $\overline{M}_w$. These measurements were expected to be underestimated due to the low resolution of the chromatographic system at the very high molar masses. A sensitivity analysis was carried out by simulating errors in the measured $\overline{M}_w$ values. First, the effects of such errors on the average branching obtained through the readjusted polymerization model $\overline{B}_{n3,theor.}$ were analyzed. Then, these values were loaded into eq. (14) to investigate their effects on the resulting ε. More specifically, variations of +20%, +10%, −10% and −20% were introduced into the measurements of $\overline{M}_w$, and their effects were observed on: (i) the new fitted values of k_{fp} [eq. (12)]; (ii) $\overline{B}_{n3,theor.}$ as predicted by the polymerization model; and (iii) the best ε value obtained by solving eq. (14) with $\overline{B}_{n3,exp.}(\varepsilon)$ obtained from the Ideal SEC/viscometry Model. The results are in Table V. It is seen that the imposed variations in $\overline{M}_w$ produce similar variations in k_{fp}. However, this is not the case for ε, where +20 and −20% variations in $\overline{M}_w$ produce −9.6 and +34.6% variations in ε. The fact that ε is less sensitive to negative variations in $\overline{M}_w$ seems convenient, since as explained before, the real measurements are expected to be in defect.

CONCLUSIONS

The unseeded batch emulsion polymerization of Is at 10°C with nDM produces broad MWDs with an essentially linear low molar mass fractions and an average branching that increases with the molar mass. The very broad MWDs obtained could be narrowed by reducing the final conversion and/or by carrying out semibatch additions of CTA.

TABLE V
Sensitivity Analysis Results

Variations in	Induce the following fractional variations in		
$\overline{M}_w$ [%]	k_{fp} [%]	$\overline{B}_{n3,theor.}$ [%]	ε [%]
−20	−25.7	26.6	34.6
−10	−11.6	14.5	17.3
+10	8.4	−5.1	−3.8
+20	16.6	−13.5	−9.6

The CTA concentration exhibited a strong effect on the MWD, a very moderate effect on the number-average degree of branching, and an almost negligible effect on the monomer conversion and particle diameter. To compensate for the diffusion-controlled nature of the chain transfer reactions to the polymer, the corresponding rate constant was assumed to depend on the observed $\overline{M}_w$ values.

The ε exponent of PI in THF at room temperature was indirectly estimated as $\varepsilon = 2.5$. To this effect, an optimization procedure was applied that forced the SEC determinations on the average degree of branching to adjust the polymerization model predictions. Finally, a sensitivity analysis demonstrated that the obtained value of ε was relatively unaffected by errors in $\overline{M}_w$.

APPENDIX: MATHEMATICAL MODEL

Basic module

From the kinetic mechanism of Table II, the following mass balances can be written:

$$\frac{dN_{Is}}{dt} = -k_p[Is]_p \frac{\overline{n} N_p}{N_A} \tag{A1}$$

$$\frac{dN_I}{dt} = -k_1 N_{Fe^{2+}}[I]_w \tag{A2}$$

$$\frac{dN_X}{dt} = -k_{fX}[X]_p \frac{\overline{n} N_p}{N_A} \tag{A3}$$

$$\frac{dN_{Fe^{2+}}}{dt} = -k_1 N_{Fe^{2+}}[I]_w + k_2 \frac{N_{Fe} - N_{Fe^{2+}}}{V_w} N_{Ra} \tag{A4}$$

$$\frac{dN_{Ra}}{dt} = -k_2 \frac{N_{Fe} - N_{Fe^{2+}}}{V_w} N_{Ra} \tag{A5}$$

$$\frac{dN_p}{dt} = \frac{A_m}{A_m + A_p} \left[k_1 N_{Fe^{2+}}[I]_w + k_{de} \frac{\overline{n} N_p}{N_A} \right] N_A \tag{A6}$$

where N_{Is}, N_I, N_X, N_{Fe}^{2+}, N_{Fe} and N_{Ra} are the moles of Is, initiator, CTA, FeSO$_4$, total Fe (Fe^{2+} and Fe^{3+}), and reducing agent, respectively; $[Is]_p$ and $[X]_p$ are the molar concentrations of Is and X in the polymer particles; $[I]_w$ is the initiator concentration in the aqueous phase; N_p is the number of polymer particles; k_p and k_{fX} are, respectively, the rate constants of propagation and of chain transfer to the CTA; k_{de} is the rate constant of $X^\bullet$ radical desorption from the polymer particles; k_1 is the rate constant for generation of primary free radicals; k_2 is the rate constant of the reduction reaction in the initiation mechanism; $\overline{n}$ is the average number of radicals per particle; N_A is the Avogadro's constant; A_m and A_p are the surface areas of micelles and polymer particles, respectively; and V_w is the aqueous phase volume.

The total volume (V_T) and the phase volumes of monomer droplets (V_d), polymer particles (V_p), and aqueous phase (V_w), were calculated through:

$$V_T = V_d + V_w + V_p \tag{A7}$$

$$V_d = \frac{M_{Is}}{\rho_{Is}} \left(N_{Is} - [Is]_p V_p - [Is]_w V_w \right) \tag{A8}$$

$$V_w = \frac{V_{H_2O}}{1 - [Is]_w \frac{M_{Is}}{\rho_{Is}}} \tag{A9}$$

$$V_p = \frac{M_{Is} N_{Is,b}}{\rho_p \phi_p} \tag{A10}$$

with

$$N_{Is,b} = N_{Is}^0 - N_{Is} \tag{A11}$$

$$\phi_p = 1 - \frac{M_{Is}[Is]_p}{\rho_{Is}} \tag{A12}$$

where N_{Is}^0 are the initial moles of Is; $N_{Is,b}$ are the bounded moles of Is; $[Is]_w$ is the molar concentration of Is in the aqueous phase; ϕ_p is the polymer volume fraction in the polymer phase; ρ_{Is} and ρ_p are, respectively, the monomer and polymer densities; M_{Is} is the monomer molar mass; and V_{H_2O} is the total water volume.

Assuming equilibrium of Is and X between phases, with constant partition coefficients, their concentrations in the polymer particles are:

$$[j]_p = \frac{N_j}{K_{jdw} K_{jwp} V_d + K_{jwp} V_w + V_p} \quad (j = Is, X) \tag{A13}$$

The unswollen particle diameter (d_p) is calculated from N_p as follows:

$$d_p = \left(\frac{6 V_{pol}}{\pi N_p} \right)^{1/3} \tag{A14}$$

and the dry polymer volume (V_{pol}) is:

$$V_{\text{pol}} = \frac{M_{\text{Is}} N_{\text{Is,b}}}{\rho_p} \tag{A15}$$

Neglecting the monomer droplets area, the total areas of polymer particles and micelles are:

$$A_p = (6\pi^{1/2} V_p)^{2/3} N_p^{1/3} \tag{A16}$$

$$A_m = A_S(N_E - [E]_{\text{CMC}} V_w) - A_p \tag{A17}$$

where A_S represents the emulsifier surface coverage capacity; N_E are the total moles of emulsifier; and $[E]_{\text{CMC}}$ is the critical micellar concentration of the emulsifier.

The average number of free-radicals per particle, $\overline{n}$, is calculated with the classical expression by Ugelstad and Hansen,[35] with the global rate of radical desorption given by[28]:

$$k_{\text{de}} = \frac{12 D_{Xw} \delta k_{fX} [X]_p K_{Xwp}}{\overline{d}_p^2 k_p [\text{Is}]_p} \tag{A18}$$

where D_{Xw} is the diffusion coefficient of $X^\bullet$ in the aqueous phase, and δ is the ratio between the mass transfer resistance of $X^\bullet$ in the aqueous phase and the overall mass transfer resistance.

The monomer conversion (x) is given by:

$$x = \frac{N_{\text{Is,b}}}{N_{\text{Is}}^0} \tag{A19}$$

Molecular weights module

For calculating the average molecular weights and degrees of branching, the termination reactions are neglected, and the dead polymer is assumed to be only generated by the transfer reactions. The following expressions are derived for the first three moments of the number chain-length distribution $(Q_0, Q_1, \text{ and } Q_2)$:

$$\frac{d(V_p Q_0)}{dt} = (k_{fM}[\text{Is}]_p + k_{fX}[X]_p - k_p^* Q_1) \frac{\overline{n} N_p}{N_A} \tag{A20}$$

$$\frac{d(V_p Q_1)}{dt} = k_p [\text{Is}]_p \frac{\overline{n} N_p}{N_A} \tag{A21}$$

$$\frac{d(V_p Q_2)}{dt} = 2(k_p [\text{Is}]_p + k_p^* Q_2)$$
$$\times \left[\frac{k_p [\text{Is}]_p + k_{fX}[X]_p + (k_{fP} + k_p^*) Q_2}{k_{fM}[\text{Is}]_p + k_{fX}[X]_p + k_{fP} Q_1} \right] \frac{\overline{n} N_p}{N_A} \tag{A22}$$

Finally, the number of tri- and tetrafunctional branches per molecule are obtained from:

$$\frac{d(V_p Q_0 \overline{B}_{n3})}{dt} = k_{fP} Q_1 \frac{\overline{n} N_p}{N_A} \tag{A23}$$

$$\frac{d(V_p Q_0 \overline{B}_{n4})}{dt} = k_p^* Q_1 \frac{\overline{n} N_p}{N_A} \tag{A24}$$

and the average molecular weights are given by:

$$\overline{M}_n = M_{\text{Is}} \frac{Q_1}{Q_0} \tag{A25}$$

$$\overline{M}_w = M_{\text{Is}} \frac{Q_2}{Q_1} \tag{A26}$$

References

1. Zubitur, M.; Ben Amor, S.; Bauer, C.; Amram, B.; Agnely, M.; Leiza, J. R.; Asua, J. M. Chem Eng J 2004, 98, 183.
2. Hamed, G. In Engineering with Rubber: How to Design Rubber Components, Gent, A.N., Ed.; Hanser Publication: New York, 2001.
3. Blackley, D. C. In Emulsion Polymerization and Emulsion Polymers, Lovell, P. A., El-Aasser, M. S., Eds.; Wiley: New York, 1997.
4. Marvel, C. S.; Williams, J. L. R. J Polym Sci 1949, 4, 265.
5. Sheinker, A. P.; Medvedev, S. S. Rubber Chem Technol 1956, 29, 121.
6. Tobolsky, A. V.; Rogers, C. E. J Polym Sci 1959, 40, 73.
7. Morton, M. P.; Salatiello, P. P.; Lanfield, H. J Polym Sci 1952, 3, 279.
8. Plessis, C.; Arzamendi, G.; Leiza, J. R.; Schoonbrood, H. A. S.; Charmot, D.; Asua, J. M. Macromolecules 2000, 33, 4.
9. Plessis, C.; Arzamendi, G.; Leiza, J. R.; Schoonbrood H. A. S.; Charmot, D.; Asua, J. M. Macromolecules 2000, 33, 5041.
10. Plessis, C.; Arzamendi, G.; Leiza, J. R.; Alberdi, J. M.; Schoonbrood, H. A. S.; Charmot, D.; Asua, J. M. J Polym Sci A Polym Chem 2001, 39, 1106.
11. Plessis, C.; Arzamendi, G.; Leiza, J. R.; Schoonbrood H. A. S.; Charmot, D.; Asua, J. M. Macromolecules 2001, 34, 5147.
12. Klimke, K.; Parkinson, M.; Piel, C.; Kaminsky, W.; Spiess, H. W.; Wilhelm, M. Macromol Chem Phys 2006, 207, 382.
13. Pollard, M.; Klimke, K.; Graf, R.; Spiess, H. W.; Wilhelm, M.; Sperber, O.; Piel, C.; Kaminsky, W. Macromolecules 2004, 37, 813.
14. Vittorias, I.; Parkinson, M.; Klimke, K.; Debbaut, B.; Wilhelm, M. Rheol Acta 2007, 46, 321.
15. Castignolles, P.; Graf, R.; Parkinson, M.; Wilhelm, M.; Gaborieau, M. Polymer 2009, 50, 2373.
16. Meira, G. R. In Modern Methods of Polymer Characterization; Barth, H. G., Mays, J., Eds.; Wiley: New York, 1991, p 67.
17. Guaita, M.; Chiantore, O. J. Liq Chromatogr 1993, 16, 633.
18. Zimm, B. H.; Stockmayer, W. H. J Chem Phys 1949, 17, 1301.
19. Stockmayer, W. H.; Fixman, M. Ann N Y Acad Sci 1953, 57, 334.
20. Zimm, B. H.; Kilb, R. W. J Polym Sci 1959, 37, 19.
21. Burchard, W. Adv Polym Sci 1999, 143, 113.
22. Vega, J.; Estenoz, D.; Oliva, H.; Meira, G. Int J Polym Anal Charact 2001, 6, 339.
23. Tackx, P.; Tacx, J. C. J. F. Polymer 1998, 39, 3109.
24. Kühn, R.; Kromer, H.; Rosmanith, G. Angew Makromol Chem 1974, 40, 361.

25. Jackson, C.; Chen, Y.; Mays, J. J Appl Polym Sci 1996, 61, 865.
26. Tung, L. J Appl Polym Sci 1979, 24, 953.
27. Gugliotta, L. M.; Brandolini, M. C.; Vega, J. R.; Iturralde, E. O.; Azum, J. M.; Meira, G. R.; Polym Reac Eng 1995, 3, 201.
28. Nomura, M.; Minamino, Y.; Fujita K. J Polym Sci Polym Chem 1982, 20, 1261.
29. Wilke, C. R.; Chang, P. C. AIChE J 1955, 1, 264.
30. Harelle, L.; Pith, T.; Hu, G.; Lambla, M. J Appl Polym Sci 1994, 52, 1105.
31. Brandrup, J.; Immergut, E. H. Polymer Handbook, 2nd edition; Wiley: New York, 1975.
32. Gangolli, S. Dictionary of Substances and Their Effects, (DOSE, 3rd Electronic Edition); Royal Society of Chemistry: Cambridge, 2005.
33. Song, Z.; Poehlein, G. W. Polym Plast Technol Eng 1990, 29, 377.
34. Nomura, M.; Suzuki, H.; Tokunaga, H.; Fujita, K. J Appl Polym Sci 1994, 51, 21.
35. Ugelstad, J.; Hansen, F. K. Rubber Chem Technol 1976, 49, 536.